Catalysis Letters 14 (1992) 207–220

Reducibility and CO hydrogenation over Pt and Pt-Co bimetallic catalysts encaged in NaY-zeolite

Genmin Lu *, Tamás Hoffer and László Guczi **

Surface Science and Catalysis Laboratory, Institute of Isotopes of the Hungarian Academy of Sciences, P.O. Box 77, H-1525 Budapest, Hungary

Received 5 February 1992; accepted 15 April 1992

Temperature programmed techniques (TPR, TPD) and X-ray diffraction (XRD) have been used to study ion migration and location as well as reducibility of platinum and cobalt ions encapsulated in Pt/NaY, Co/NaY and Pt-Co/NaY zeolites prepared by ion exchange. The temperature required to reduce Co^{2+} in NaY was significantly lowered by the presence of Pt and dependent upon the relative locations of Pt and Co ions in zeolite cages. The exact location was controlled by the calcination condition and the metal contents. For bimetallic catalyst with low Pt content (0.5 wt% Pt and 0.9 wt% Co), the TPR results indicated that reduction of Co^{2+} ions in the vicinity of Pt shifted toward lower temperature, while that of Co^{2+} staying alone was not affected. With high Pt loading (4.5 wt% Pt, 0.7 and 2.6 wt% Co), however, most of the Co^{2+} ions were reduced by means of Pt at temperature below 723 K after calcination at 573 K. The temperature for Pt reduction in bimetallic catalysts was somewhat higher than Pt/NaY and increased with Co atomic fraction, indicating that mixed oxide, $PtCo_xO_y$, might be formed during calcination. After reduction in hydrogen at 723 K, highly dispersed metal particles were formed. These fine particles were most probably confined inside zeolite cages as indicated by the absence of XRD peak for all samples after calcination and reduction. Surface composition of the bimetallic particles may be different for catalysts with similar Pt content but different Co loading. Accordingly, H/Pt ratios of 1.0 and 0.72 for catalysts with low and high Co content, respectively, were shown by hydrogen chemisorption. It was further supported by the increase in TPD peak intensity with Co loading in the high temperature range, which was related to the reoxidation of Co in bimetallic particles by surface hydroxyl groups. Preliminary results on CO hydrogenation demonstrated that activity and methanol selectivity were higher on Pt-Co bimetallic catalysts than either over monometallic Pt or Co catalyst, which was consistent with the Pt enhanced Co reduction and formation of Pt-Co bimetallic particles.

Keywords: Pt/NaY; Pt-Co/NaY; ion exchange; temperature programmed reduction and desorption; X-ray diffraction; Pt-Co bimetallic particles; H_2 chemisorption; CO hydrogenation

* Permanent address: Institute of Coal Chemistry, Chinese Academy of Sciences, Taiyuan, Shanxi 030001, PR China.

** To whom correspondence should be addressed.

1. Introduction

Combination of the traditional Fischer–Tropsch synthesis catalysts (Fe, Co) with metals of good hydrogenation activity, e.g., Pt, Ir, or Pd, on which CO do not easily dissociate, could lead to catalysts being the most appropriate for synthesis of oxygenates, particularly methanol [1]. Introduction of zeolite into this system may further enhance oxygenate formation by confining metal particle size and stabilizing its state through the zeolite framework [2,3]. Zeolite encaged bimetallic catalyst, therefore, appears to be promising for alcohol synthesis from syngas.

Previous works in our laboratory on Pd and Pd based bimetallic catalysts supported on NaHX-zeolite [4–7] have indicated that the activity and selectivity of Pd for methanol formation from CO hydrogenation could be dramatically enhanced by iron and/or La. In the case of PdFe/NaHX-zeolite the formation of bimetallic $PdFe_x$ particles inside the zeolite cages was evidenced from Mössbauer spectroscopy [5,6]. The promotion by Fe was considered as modifying the Pd for both dissociative/associative CO adsorption and for weakly/strongly adsorbed hydrogen [8].

However, transition metals such as Fe and Co with large negative electrochemical potentials are very difficult to reduce in zeolite. This low reducibility may, in turn, influence the formation of bimetallic particles, which is prerequisite for the formation of bimetallic catalysts. The reoxidation of finely dispersed particles by reaction with surface hydroxyl groups may not be excluded, either [9].

Reducibility of the transition metal cations in zeolite is highly dependent on their location and chemical states, which can be controlled by catalyst preparation and pretreatment. The presence of readily reducible metal can catalyze the reduction of less reducible metal. Zhang et al. [10,11] found that the temperature for Co^{2+} ion reduction in NaY was lowered by the presence of Pd, if Pd^{2+} and Co^{2+} ions remained in the same cage after calcination. Percentage of the reduced Co was controlled by the calcination temperature and the Co precursor applied for ion exchange.

Table 1
Metal content in catalysts measured by XRF

No.	Catalyst	Pt (wt%)	Co (wt%)	Co/(Pt+Co)
(I)	$Pt_{1.2}NaY$	1.2	–	0
	$Pt_{0.5}Co_{0.9}NaY$	0.5	0.9	0.86
	$Co_{1.4}NaY$	–	1.4	1.0
(II)	$Pt_{6.5}NaY$	6.5	–	0
	$Pt_{4.3}Co_{0.7}NaY$	4.3	0.7	0.34
	$Pt_{4.6}Co_{2.6}NaY$	4.6	2.6	0.65
	$Co_{5.6}NaY$	–	5.6	1.0

Although combination of the Pt and Co metals supported on certain oxide supports has been found to produce alcohols from syngas [1,12], little is known about the reducibility and interaction of metals in Pt-Co/NaY-zeolite. In the present paper temperature programmed reduction and desorption (TPR, TPD), X-ray diffraction (XRD) as well as preliminary results on CO hydrogenation to methanol are applied to study the ion reducibility and the surface properties of metal particles in Pt/NaY, Co/NaY and Pt-Co/NaY catalysts.

2. Experimental

2.1. CATALYST PREPARATION

The Pt/NaY, Co/NaY and bimetallic Pt-Co/NaY zeolites were prepared by ion exchange. NaY zeolite (Strem Chemicals, Lot No. 031112104) was first stirred with doubly deionized water (200 ml/g zeolite) at 343 K for 1 h. A dilute aqueous solution of $Pt(NH_3)_4(NO_3)_2$ or $Co(NO_3)_2$ (2×10^{-2} mol/cm^3) was added dropwise to the zeolite slurry under stirring at 343 K. The pH of the slurry was set to a final value of 6.5. After 24 h ion exchange at the same temperature, the catalyst was filtered and thoroughly washed with deionized water. For preparation of the Pt-Co/NaY bimetallic catalyst, Pt^{2+} was introduced first, then after filtering, the Pt/NaY was further exchanged with Co^{2+} solution. All catalysts were dried in air first at room temperature (RT) and then at 383 K for 2 h.

Pt and Co contents in the catalysts were determined by X-ray fluorescence (XRF) and the results are given in table 1. Two series of catalysts with low and high metal contents were prepared. Samples with different metal contents are designated according to table 1 where the subscripts represent the weight percent of the respective metal in the zeolite samples.

2.2. TEMPERATURE PROGRAMMED REDUCTION AND DESORPTION

Temperature programmed experiments were conducted in a flow apparatus equipped with a thermal conductivity detector (TCD) and a quadrupole mass spectrometer (QMS). 0.03–0.10 g catalyst was first calcined for 2 h in flowing oxygen with 40 cm^3/min flow rate, while the temperature raised from RT to the desired value at a rate of 0.5 K/min. After purging with Ar for 1 h at the calcination temperature, the sample was cooled in Ar to RT for the TPR experiment. TPR was performed using 1% H_2 in Ar (30 cm^3/min) with 10 K/min ramp rate. At the final temperature, the H_2/Ar mixture was replaced first by pure H_2 for 1 h, then by Ar for 1 h. The reduced sample was cooled in Ar to RT for H_2 pulse adsorption, which was followed by TPD in Ar (20 cm^3/min) with 20 K/min. Before TPR, H_2 consumption of the calcined sample

at RT was measured by H_2 pulse in Ar the amount being around 10% of the total H_2 consumption, was added to the amount from TPR for total H_2 consumption calculation.

2.3. X-RAY DIFFRACTION

The XRD pattern was recorded by using Cu K_α radiation on a Philips X-ray diffractometer equipped with a Guiner camera. The catalysts were first treated in a similar procedure as in TPR or CO hydrogenation. Samples were cooled in Ar to RT and then passivated for XRD measurements. The parent NaY zeolite was used as reference for peak assignment. All catalysts of series (I) and (II) after 573 K calcination and 723 K reduction as well as $Pt_{4.6}Co_{2.6}NaY$ after 573 K calcination were examined. However, no apparent diffraction peak other than zeolite itself was detected for the samples. The XRD spectrum is, therefore, not presented in the paper. The maximum particle size was estimated to be less than 2.5–3.0 nm based on the experimental condition applied in the present study.

2.4. $CO+H_2$ REACTION

Preliminary experiments on the CO hydrogenation over catalysts of series (II) were performed in a stainless steel tubular reactor charged with 0.15 g catalyst

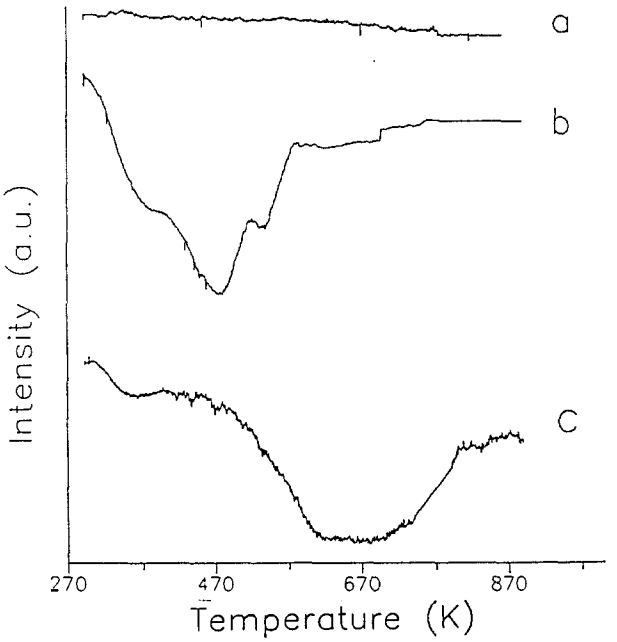

Fig. 1. TPR profiles of NaY (a) and $Pt_{1.2}NaY$ (b, c) after calcination at 573 K (a); 573 K (b); and 723 K (c).

between two plugs of quartz wool. The catalyst was calcined in flowing O_2 at 573 K for 2 h by a similar procedure as in TPR. To facilitate Co reduction, the calcined catalyst was reduced at 723 K for 24 h with 4 bar H_2 (30 cm^3/min). The reduced catalyst was cooled in H_2 to reaction temperature. After having the H_2 replaced gradually by the $CO + H_2$ mixture, the pressure was adjusted to 10 bar. Temperature was controlled with a precision of 2 K. Premixed feed gas with $CO/H_2 = 0.5$ was purified by passing through activated carbon, prereduced manganese acetate on molecular sieve and finally through silica gel. The flow rate was controlled by a valve for 15 cm^3/min. Effluent gas was sampled by a six-port valve through heated line and analyzed by using an on-line Parkard-437 gas chromatograph. Separation was carried out using a Chromsorb 101 column for alcohols and a *n*-octane/Parasil-C column for hydrocarbon. Activity and selectivity were defined in terms of carbon balance. The total reaction rate was calculated from CO consumption with exclusion of CO_2 formation and was expressed in mol/s/mol-metal unit. The steady-state reaction was established after 1 h on stream and the result after 2 h reaction was used for activity and selectivity calculation.

3. Results and discussion

3.1. TPR ON CATALYSTS OF SERIES (I)

TPR profiles for the catalysts of series (I) which were calcined at different temperatures, are shown in figs. 1–3. It can be seen from fig. 1b that on $Pt_{1.2}NaY$, after calcination at 573 K, the main TPR peak appears at 473 K along with shoulders at 383 and 531 K. However, after calcination at 723 K, a broad peak is found between 623 and 723 K. No measurable hydrogen consumption was detected for NaY calcined at 573 K (fig. 1a). The influence of calcination temperature on TPR profile was investigated in the temperature range between 523 and 773 K. The results indicate shifts for the TPR peaks toward higher temperature with increasing calcination temperature. The H_2 consumption calculated from each TPR curve indicates that about one hydrogen molecule is consumed per Pt ion as shown in table 2. This implies that most of Pt remain in divalent state after calcination.

The ion location in Pt/NaY and its reducibility have been extensively studied by Gallezot et al. [13] with XRD and Sachtler and co-workers [14] with temperature programmed techniques. The present results are consistent with that of these authors and a similar conclusion can be drawn from fig. 1. After calcination at 573 K most of Pt^{2+} ions remain in the supercages and are reduced at lower temperature. With increasing calcination temperature, Pt^{2+} is gradually driven into the small sodalite cages where higher reduction temperature is required. Fig. 1c indicates that after calcination at 723 K, most of Pt^{2+} may be

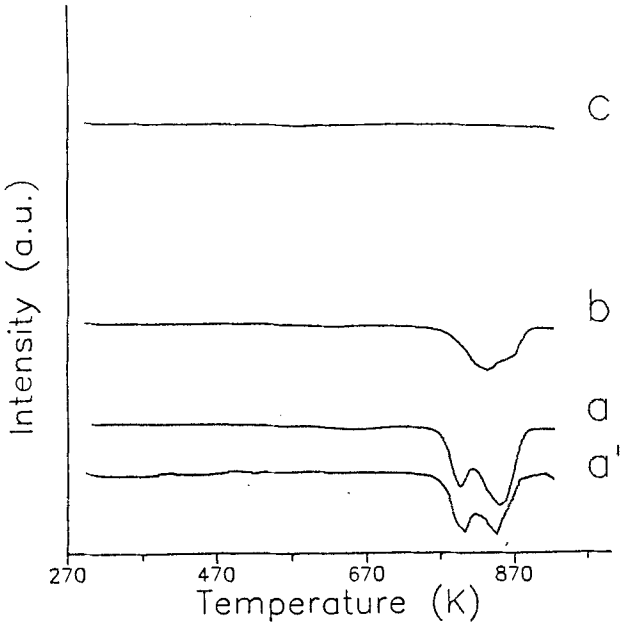

Fig. 2. TPR profiles of $Co_{1.4}NaY$ after calcination at RT (a'); 573 K (a); 723 K (b); and 773 K (c).

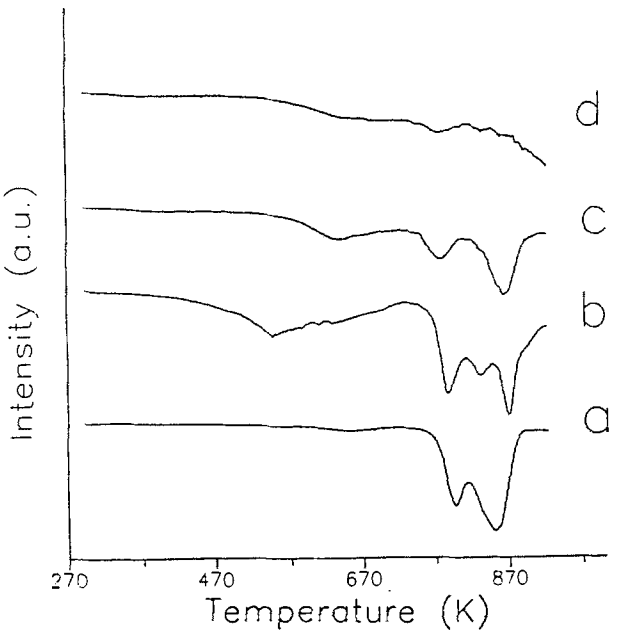

Fig. 3. TPR profiles of $Pt_{0.5}Co_{0.9}NaY$ (b, c, d) and $Co_{1.4}NaY$ (a) after calcination at 573 K (a) (fig. 2a); 573 K (b); 723 K (c); and 773 K (d).

Table 2
H_2 consumption [H_2/(Pt+Co)] in TPR and Pt dispersion (H/Pt)

Catalyst	Calcination temperature	H_2(TPR) [a] /(Pt+Co)	H/Pt [b]	H_2(TPD) [d] /(Pt+Co)
$Pt_{1.2}NaY$	573	1.2	1.1	
	723	1.2	0.3	
$Pt_{0.5}Co_{0.9}NaY$	573	1.04	0.92	
	723	0.70	0.35	
	773	0.64	–	
$Co_{1.4}NaY$	573	0.60	–	
	723	0.29	–	
	773	0	–	
$Pt_{6.5}NaY$	573	1.08	0.83	0.05
$Pt_{4.3}Co_{0.7}NaY$	573	1.73	1.20 (0.97) [c]	0.14
$Pt_{4.6}Co_{2.6}NaY$	573	0.88	0.72 (0.72) [c]	0.24
$Co_{5.6}NaY$	573	0.25	–	

[a] TPR to 923 K.
[b] TPR to 723 K, reduction with H_2 for 1 h.
[c] O_2–H_2 titration at RT.
[d] H_2 evolved in TPD at high temperature (see fig. 5).

located in the sodalite cages with a minor part left in the supercages.

Metal dispersion is largely dependent on the location of Pt^{2+} in zeolite. For Pt dispersion measurement the TPR was stopped at 723 K and the catalyst was further reduced with pure H_2 at this temperature for 1 h. H_2 adsorption was measured at RT to determine the H/Pt ratio. Table 2 demonstrates that calcination at 573 K followed by 723 K reduction results in optimum dispersion (H/Pt $\approx$ 1.0) for $Pt_{1.2}NaY$. The absence of the XRD peak presented further evidence indicating that highly dispersed Pt particles were formed inside zeolite cages. It was reported that complete decomposition of $Pt(NH_3)_4^{2+}$ could be achieved only at temperature higher than 573 K. Lower calcination temperature, e.g. 523 K, also resulted in low dispersion due to formation of neutral $Pt(NH_3)_2H_2$ species during reduction of incompletely decomposed sample [15].

TPR spectra of the $Co_{1.4}NaY$ sample are shown in fig. 2. At temperature below 723 K, no Co reduction peak was found with different calcination temperatures. In the high temperature range, two peaks appear at 803 and 843 K (figs. 2a′ and 2a). The peak positions are nearly the same after RT (fully hydrated, fig. 2a′) and 573 K calcination, while the relative intensity of the peak at 803 K is somewhat diminished compared to that observed at 843 K. The total H_2 consumption decreases with increasing calcination temperature (table 2).

After calcination at 773 K, all peaks below 923 K have vanished (fig. 2c). Hutta and Lunsford [16] found by DRS that fully hydrated $Co(H_2O)_6^{2+}$ ions were located in the supercages of NaY, while most of Co^{2+} migrated into sodalite cages after evacuation at 573 K. The only detectable Co species in the $Co_{1.4}NaY$ sample is Co^{2+} ions measured by XPS, either after drying at 383 K or calcination at 573 K. The reduction peaks in fig. 2a can, therefore, be attributed to different Co^{2+} in small cages as a result of migration from supercages during calcination (fig. 2a) or reduction (fig. 2a'). The change in relative peak intensities indicates migration of Co^{2+} ions to more hidden sites with increasing calcination temperature. As a result, the relative amount of reducible Co^{2+} ions decreases, and the reduction peak disappears completely after 773 K calcination.

The TPR profiles for $Pt_{0.5}Co_{0.9}NaY$ catalyst are illustrated in fig. 3. For comparison the TPR curve of $Co_{1.4}NaY$ calcined at 573 K (fig. 2a) is replotted in fig. 3a. After calcination at 573 K, the low temperature peak around 503 K in fig. 3b can be assigned to the reduction of Pt in supercages as for $Pt_{1.4}NaY$ in fig. 1b. The triplet peak in high temperature range can be considered as reduction of Co species in small cages. The first peak shifts toward lower temperature compared with $Co_{1.4}NaY$ and the temperature further decreases with increasing calcination temperature. On the other hand, after calcination at 723 K the second and the third peaks merge into one peak with the position similar to the second peak in fig. 3a for $Co_{1.4}NaY$.

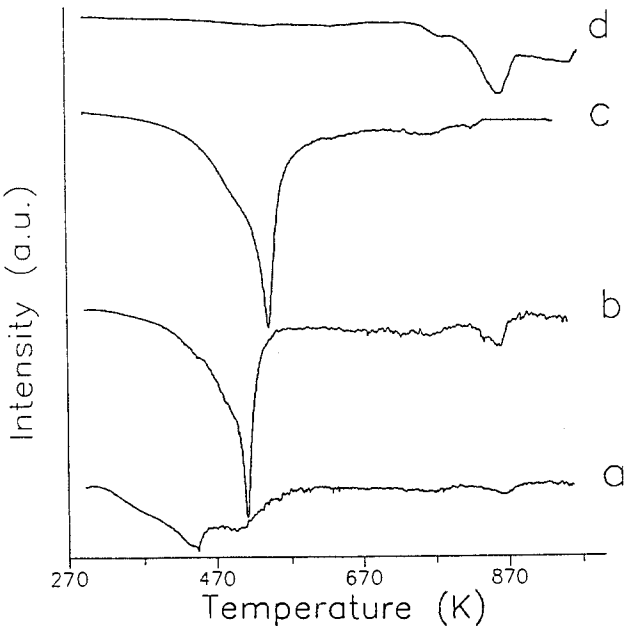

Fig. 4. TPR profiles of catalysts after calcination at 573 K. $Pt_{6.5}NaY$ (a); $Pt_{4.3}Co_{0.7}NaY$ (b); $Pt_{4.6}Co_{2.6}NaY$ (c); and $Co_{5.6}NaY$ (d).

By comparison with TPR results in figs. 1 and 2 for Pt/NaY and Co/NaY catalysts, respectively, the first peak in the triplet of fig. 3b can be assigned to the reduction of Co in the vicinity of Pt in small cages. With increasing calcination temperature Pt are gradually driven into small cages. At the same time, more Co migrate to the hidden sites. Therefore the position of this peak shifts to lower temperature due to the presence of Pt to catalyze Co reduction. The second and the third peaks may be considered as the reduction of Co alone, which is probably located at the same position as Co reduced in the second peak in fig. 3a for $Co_{1.4}NaY$. The lower Co content in $Pt_{0.5}Co_{0.9}NaY$ results in better curve resolution in fig. 3b, while fig. 3a presents a broader peak for $Co_{1.4}NaY$.

The enhancement of Co reduction in $Pt_{0.5}Co_{0.9}NaY$ is remarkable considering the low average cage sharing of Pt and Co atoms in this catalyst (< 1 atom/u.c.), especially after 573 K calcination which may put very small amount of Pt in sodalite cages. This indicates that the migration of ions or particles results in interaction of Pt and Co in the zeolite cages. It should be mentioned that although $H_2/(Pt + Co)$ in TPR for $Pt_{0.5}Co_{0.9}NaY$ after 573 K calcination is around 1.0 (table 1), this may not indicate the complete reduction of Co in the catalyst because reduction of only a part of Co is catalyzed by Pt.

3.2. TPR AND TPD ON CATALYSTS OF SERIES (II)

To further investigate the enhancement of Co reduction by Pt, catalysts of series (II) with high metal loading are characterized by TPR and TPD of adsorbed hydrogen after calcination at 573 K. As shown in fig. 4a, reduction of $Pt_{6.5}NaY$ is completed at temperature below 723 K. H_2 consumption per Pt atom is again 1.0 similarly to what was observed for $Pt_{1.4}NaY$. The TPR curve for $Co_{5.6}NaY$ (fig. 4d) is similar to $Co_{1.4}NaY$ in fig. 2a. Negligible H_2 consumption is measured at temperature below 573 K. The main peak for Co reduction appears at 853 K with a small shoulder around 783 K. When TPR is performed on $Pt_{4.3}Co_{0.7}NaY$ and $Pt_{4.6}Co_{2.6}NaY$ bimetallic catalysts, the profiles are remarkably different from both $Pt_{6.5}NaY$ and $Co_{5.6}NaY$ as shown in figs. 4b and 4c, respectively. Reduction of Pt and Co merges into one peak with T_{max} at 513 and 543 K for $Pt_{4.3}Co_{0.7}NaY$ and for $Pt_{4.6}Co_{2.6}NaY$, respectively. In addition, a minor separate peak is also found in the high temperature range. The results clearly demonstrate that most of Co ions are co-reduced with Pt at temperature below 723 K in these two catalysts.

It is worth mentioning that the reduction temperature for $Pt_{4.6}Co_{2.6}NaY$ is higher than $Pt_{4.3}Co_{0.7}NaY$, and both are higher than that for $Pt_{6.5}NaY$. Because Pt contents in both bimetallic catalysts are nearly the same, the higher reduction temperature with high Co loading may be due to more remarkable interaction between Pt and Co or formation of mixed oxides with different composition during calcination mainly in the supercage. Higher reduction temperature for Pt in bimetallic catalysts compared to that for $Pt_{6.5}NaY$ is the second indication for

the formation of bimetallic oxide particles. Interaction of Pt and Co precursors or formation of Pt-Co mixed oxide particles during calcination prevents migration of Co ions into small cages and leads to co-reduction of most Co with Pt at lower temperature in supercages. This is apparently different from $Pt_{0.5}Co_{0.9}NaY$ shown in fig. 3 where Pt catalyzed Co reduction occurs at higher temperature, indicating the different locations of bimetallic particles in these two catalysts. Park et al. [17] also found that the Pt reduction temperature in PtFe/NaY shifted to higher temperature due to formation of $PtFe_xO_y$ mixed oxide particles.

As far as the mechanism for $PtCo_xO_y$ particles formation is concerned, one possible way is the reaction of Pt^{2+} and Co^{2+} ions with water adsorbed in zeolite or formed during calcination in O_2. This reaction will produce protons to occupy the cation sites in the zeolite. H_2 consumption during TPR (table 2) for $Pt_{4.3}Co_{0.7}NaY$ far exceeds 1.0 indicating oxidation of Co and/or Pt to higher valence during calcination. For $Pt_{4.6}Co_{2.6}NaY$ catalyst, $H_2/(Pt + Co) = 0.88$ implies that a part of Co are not reduced below 923 K. Because of the higher atomic fraction of Co in this catalyst, the non-reduced Co may stay alone in small cages.

For metal dispersion measurements, TPR is stopped at 723 K. As shown in table 2, the H/Pt ratio of 0.83 was measured on $Pt_{6.5}NaY$. The H/Pt ratios for $Pt_{4.3}Co_{0.7}NaY$ and $Pt_{4.6}Co_{2.6}NaY$ are 1.2 and 0.72, respectively.

To eliminate the influence of Co on the dispersion measurement of Pt, preliminary experiments on O_2–H_2 titration at RT were also performed for bimetallic catalysts. $H/Pt = 0.97$ and 0.72 are found for $Pt_{4.3}Co_{0.7}NaY$ and $Pt_{4.6}Co_{2.6}NaY$, respectively (table 2). The discrepancy between H_2 adsorption and O_2–H_2 titration for $Pt_{4.3}Co_{0.7}NaY$ indicates that H atoms adsorbed on Pt may migrate onto Co atoms resulting in higher H/Pt ratio, whereas in O_2–H_2 titration only the oxygen adsorbed on Pt can be titrated by H_2 at RT. However, this effect is negligible on $Pt_{4.6}Co_{2.6}NaY$. The second possibility is the change of O_2 adsorption properties with different surface composition of the bimetallic particles. The detailed results will be reported in a separate paper.

The different adsorption properties along with the different TPR characteristics of the $Pt_{4.3}Co_{0.7}NaY$ and $Pt_{4.6}Co_{2.6}NaY$ catalysts can be interpreted as follows. As found from TPR, interaction between Pt and Co or formation of $PtCo_xO_y$ mixed oxide particles occurs already during calcination. With low calcination temperature (573 K), Co in mixed oxide remains in supercages with Pt. The rest of Co ions migrate into small cages. Because the Pt contents in the two catalysts are similar, higher Co content will result in the formation of bimetallic oxide particles with higher Co fraction. After reduction, Pt-rich and Co-rich bimetallic particles are formed for the $Pt_{4.3}Co_{0.7}NaY$ and $Pt_{4.6}Co_{2.6}NaY$ catalysts, respectively. The metal particles are most probably accommodated in supercages as shown by XRD and chemisorption results. For Pt-rich particles, most of the Pt atoms are available for H_2 adsorption as indicated by the high

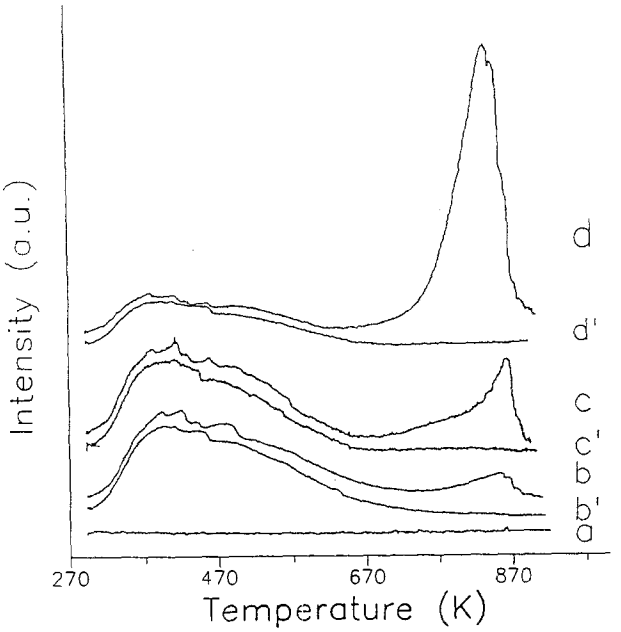

Fig. 5. TPD profiles of $Co_{5.6}NaY$ (a), $Pt_{6.5}NaY$ (b, b'), $Pt_{4.3}Co_{0.7}NaY$ (c, c') and $Pt_{4.6}Co_{2.6}NaY$ (d, d') after calcination at 573 K and reduction at 723 K. (a, b, c, d) first TPD run; (a, b', c', d'') second TPD run.

H/Pt ratio in O_2–H_2 titration. On the other hand, a part of the Pt surface is covered by Co in Co-rich particles. H_2 adsorption is diminished because Co is unable to adsorb H_2 at room temperature. Moretti and Sachtler [18] have reported a similar effect of Cu on Pt dispersion in PtCu/NaY catalyst. It is of interest to note that the present results are also consistent with the bimetallic particle model of Pt-Co/Al_2O_3 measured by XPS [12,19,20], although the extent of Co reduction may be different in these two catalyst systems.

Formation of the different bimetallic particles is further supported by the TPD of adsorbed H_2. In fig. 5 two TPD curves for each catalyst are illustrated. The first curve is recorded immediately after H_2 adsorption at RT on the catalyst reduced at 723 K. The adsorbed H_2 is desorbed in Ar in the TPD run carried out up to 923 K. Then the catalyst is cooled in Ar to RT. After H_2 adsorption, TPD is repeated on the same catalyst to measure the second curve. It can be seen from fig. 5 that the TPD curves in the first run have two peaks at temperatures below and above 723 K on all catalysts except $Co_{5.6}NaY$. The amount of H_2 under the second peak increases in the order $Pt_{6.5}NaY < Pt_{4.3}Co_{0.7}NaY < Pt_{4.6}Co_{2.6}NaY$ as shown in the last column of table 2 by H_2(TPD)/(Pt + Co). The high temperature peak disappears in the second TPD run, while the low temperature peak is similar to the first TPD curve in the same temperature range. The amount of H_2 desorbed from the low temperature

peak in the first and second TPD run are the same and also agree with H_2 adsorption at RT. Tzou et al. [21] attributed the high temperature peaks in Pt/NaY and PtFe/NaY catalysts to the reoxidation of reduced Pt atoms in sodalite cages by surface hydroxyl groups formed during reduction of the metal cations. Zhang et al. [21], however, reported the oxidative leaching of Cu in $PdCu_x$ bimetallic particles in supercages of NaY during TPD in Ar. In the present study, Pt is mainly located in supercages for both Pt/NaY and Pt-Co/NaY bimetallic catalysts after 573 K calcination. It seems that the small high temperature peak in fig. 5b for $Pt_{6.5}NaY$ can be attributed to the oxidation of Pt in sodalite cages with hydroxyl groups. If we assume that reoxidation of bimetallic catalysts had occurred also in sodalite cages, the increasing intensity of the high temperature peak with Co loading may indicate that more Co ions had been reduced in the small cages. But TPR results in fig. 4 only show a minor peak in the high temperature range. Therefore for bimetallic catalysts, in addition to the oxidation of a very small amount of reduced Pt and Co in sodalite cages, the high temperature peaks in figs. 5c and 5d are mainly due to the reoxidation of Co in $PtCo_x$ bimetallic particles in the supercages. The increasing amount of evolved H_2 with higher Co loading are consistent with TPR and chemisorption results, indicating the formation of bimetallic particles with different Co composition after reduction.

3.3. $CO+H_2$ REACTION ON CATALYSTS OF SERIES (II)

The interaction of Pt and Co in bimetallic catalysts could influence the catalytic activity and selectivity. Preliminary $CO + H_2$ reaction is investigated on catalysts of series (II). The preliminary results summarized in table 3 indicate that the activity for CO conversion, based on mol/s/mol-metal, is higher on bimetallic catalysts than either monometallic Pt or Co catalyst, and the most active catalyst is $Pt_{4.3}Co_{0.7}NaY$. This can be attributed to the co-reduction of Co with Pt and formation of Pt-Co bimetallic particles as discussed previously for TPR and TPD results. The low activity of Pt catalyst is due to its intrinsic low ability for CO activation, while the low activity of pure Co catalyst results from its low reducibility. For $Pt_{4.3}Co_{0.7}NaY$ and $Pt_{4.6}Co_{2.6}NaY$, the differences in metal dispersion and particle composition may be responsible for their different activity. But the influences of reduction extent and the surface properties of these catalysts on the reaction should be further studied.

The selectivity for methanol formation follows the same pattern. Although Pt catalyst is active for methanol formation with its ability for associative adsorption of CO, the high methanation and hydrogenation activity result in low overall methanol selectivity. For $Co_{5.6}NaY$, low methanol selectivity is related to its dissociative adsorption of CO and high activity for hydrocarbon formation. The methanol selectivity is again the highest on $Pt_{4.3}Co_{0.7}NaY$. The results are fully in agreement with the Pt-rich and Co-rich bimetallic particle model. On

Table 3
Preliminary results on CO hydrogenation over catalysts of series (II) [a]

Catalyst [b]	Rate ($\times 10^{-4}$ mol/s/mol-metal)				
	total	CH_3OH	CH_4	C_{2+}	olefin [d]
$Pt_{6.5}NaY$	4.50	1.73	1.85	0.62	
$Pt_{4.3}Co_{0.7}NaY$	6.07	4.48	0.70	0.55	
$Pt_{4.6}Co_{2.6}NaY$	3.98	1.95	0.98	0.81	
$Co_{5.6}NaY$	0.42	0.19	0.13	0.08	
	Selectivity (%)				
	Oxyg. [c]	CH_3OH	CH_4	C_{2+}	olefin [d]
$Pt_{6.5}NaY$	14.1	39.3	41.2	5.40	11.0
$Pt_{4.3}Co_{0.7}NaY$	11.1	73.8	11.5	3.60	20.1
$Pt_{4.6}Co_{2.6}NaY$	11.6	48.9	24.5	12.0	22.1
$Co_{5.6}NaY$	10.1	44.0	32.5	13.4	42.8

[a] Reaction condition: 10 bar, 505 K, 15 cm^3/min. After 2 h reaction.
[b] Pretreatment: calcination at 573 K for 2 h; reduction with 4 bar H_2 at 723 K for 24 h.
[c] Oxygenates other than methanol.
[d] Olefin selectivity in hydrocarbon products.

Pt-rich particles, highly dispersed Pt and enhanced Co reduction result in high activity, while the property of Co-rich particles is more similar to Co catalyst. The modification of Pt by Co is also evidenced from olefin selectivity in hydrocarbon products. The hydrogenation activity of Pt is diminished by the presence of Co. As a result, olefin selectivity increases with Co fraction. The formation of other oxygenates, mainly dimethyl ether (DME) under steady-state reaction, is the indication of the presence of surface acidic sites, which is formed with metal oxide formation during calcination or by cation reduction and catalyze the secondary reaction of methanol.

Finally, the XRD results show that even with prolonged hydrogen reduction and CO hydrogenation reaction, migration of metal particles inside zeolite cages onto external surface and coalescence to large particles is not appreciable for all the catalysts of series (II). Metal particle size and its state are, therefore, confined by NaY-zeolite cages.

4. Conclusions

In conclusion, the present TPR and TPD results along with XRD and chemisorption provide strong evidence for the interaction of Pt and Co to form bimetallic catalysts in the zeolite cage and this results in high activity and selectivity of the bimetallic catalysts for CO hydrogenation toward methanol.

The Co reducibility can be dramatically enhanced by the presence of Pt in the same zeolite. This enhancement depends on the calcination temperature and

metal content, which determine the relative locations of Pt and Co in zeolite. Therefore for $Pt_{4.3}Co_{0.7}NaY$ and $Pt_{4.6}Co_{2.6}NaY$ catalysts calcined at 573 K, most of Co are co-reduced with Pt at temperature below 723 K. Formation of $PtCo_xO_y$ oxide particles, which prevents Co migration into small cages, seems to be necessary for Pt catalyzed Co reduction. Pt surface properties in bimetallic catalysts can be modified by Co. With lower Co fraction, the interaction leads to the synergetic effect of Pt and Co with high activity and selectivity for methanol formation. With higher Co fraction, a part of Pt surface may be covered with Co resulting in low H_2 adsorption and methanol selectivity.

Acknowledgement

The work was supported by the Hungarian Research Fund (OTKA Grant No: 1887). The authors thank Dr. E. Zsoldos for XRD measurement.

References

[1] J.W. Niemantsverdriet, S.P.A. Louwer, J. van Grondelle, A.M. van der Kraan, F.W.H. Kampers and D.C. Koningsberger, *Proc. 9th Int. Cong. Catal.*, Vol. 2, eds. M.J. Phillips and M. Ternan (The Chemical Institute, Ottawa, 1988) p. 674.
[2] M. Ichikawa, A. Fukuoka and T. Kimura, *Proc. 9th Int. Cong. Catal.*, Vol. 2, eds. M.J. Phillips and M. Ternan (The Chemical Institute, Ottawa, 1988) p. 569.
[3] W.M.H. Sachtler, F.A.P. Cavalcanti and Z.-C. Zhang, Catal. Lett. 9 (1991) 261.
[4] B.M. Choudary, K. Lázár, K. Matusek and L. Guczi, J. Chem. Soc. Chem. Comm. (1988) 592.
[5] K. Lázár, B.M. Choudary and L. Guczi, Hyperfine Interactions 46 (1989) 591.
[6] B.M. Choudary, K. Lázár, I. Bogyai and L. Guczi, J. Chem. Soc. Faraday Trans. I 86 (1990) 419.
[7] B.M. Choudary, K. Matusek, I. Bogyay and L. Guczi, J. Catal. 122 (1990) 320.
[8] L. Guczi, Catal. Lett. 7 (1990) 205.
[9] Z.-C. Zhang, L.-Q. Xu and W.M.H. Sachtler, J. Catal. 131 (1991) 502.
[10] Z.-C. Zhang, W.M.H. Sachtler and S.L. Suib, Catal. Lett. 2 (1989) 395.
[11] Z.-C. Zhang and W.M.H. Sachtler, J. Chem. Soc. Faraday Trans. I 86 (1990) 2313.
[12] L. Guczi, T. Hoffer, Z. Zsoldos, S. Zyade, G. Maire and F. Garin, J. Phys. Chem. 95 (1991) 802.
[13] P. Gallezot, A. Alarcon-Diaz, A.-A. Delmon, A.J. Renouprez and B. Imelik, J. Catal. 39 (1975) 334.
[14] S.T. Homeyer and W.M.H. Sachtler, in: *Zeolites: Facts, Figures, Future*, eds. P.A. Jacobs and R.A. van Santen (Elsevier, Amsterdam, 1989) p. 975, and references therein.
[15] R.A. Dalla Betta and M. Boudart, *Proc. 5th. Int. Cong. Catal.*, Vol. 2 (1973) p. 1329.
[16] P.J. Hutta and J.H. Lunsford, J. Chem. Phys. 66 (1977) 4716.
[17] S.H. Park, M.S. Tzou and W.M.H. Sachtler, Appl. Catal. 24 (1986) 85.
[18] G. Moretti and W.M.H. Sachtler, J. Catal. 15 (1989) 205.
[19] Z. Zsoldos, T. Hoffer and L. Guczi, J. Phys. Chem. 95 (1991) 798.
[20] Z. Zsoldos and L. Guczi, J. Phys. Chem., submitted.
[21] M.S. Tzou, B.K. Teo and W.M.H. Sachtler, J. Catal. 113 (1988) 220.